ARTICLES

Journal of Semiconductors
(2023) 44, 082901
doi: 10.1088/1674-4926/44/8/082901

Terahertz phononic crystal in plasmonic nanocavity

Zhenyao Li[1, 2], Haonan Chang[1, 2], Jia-Min Lai[1, 2], Feilong Song[1, 2], Qifeng Yao[3], Hanqing Liu[1, 2], Haiqiao Ni[1, 2, 4], Zhichuan Niu[1, 2, 4], and Jun Zhang[1, 2, 3, †]

[1]State Key Laboratory of Superlattices and Microstructures, Institute of Semiconductors, Chinese Academy of Sciences, Beijing 100083, China

[2]Center of Materials Science and Optoelectronics Engineering, University of Chinese Academy of Sciences, Beijing 100049, China

[3]Beijing Academy of Quantum Information Sciences, Beijing 100193, China

[4]Joint Laboratory of Advanced Semiconductor, Nanjing Guoke Semiconductor CO., Ltd, Nanjing 210000, China

Abstract: Interaction between photons and phonons in cavity optomechanical systems provides a new toolbox for quantum information technologies. A GaAs/AlAs pillar multi-optical mode microcavity optomechanical structure can obtain phonons with ultra-high frequency (~THz). However, the optical field cannot be effectively restricted when the diameter of the GaAs/AlAs pillar microcavity decreases below the diffraction limit of light. Here, we design a system that combines Ag nanocavity with GaAs/AlAs phononic superlattices, where phonons with the frequency of 4.2 THz can be confined in a pillar with ~4 nm diameter. The Q_c/V reaches 0.22 nm^{-3}, which is ~80 times that of the photonic crystal (PhC) nanobeam and ~100 times that of the hybrid point-defect PhC bowtie plasmonic nanocavity, where Q_c is optical quality factor and V is mode volume. The optomechanical single-photon coupling strength can reach 12 MHz, which is an order of magnitude larger than that of the PhC nanobeam. In addition, the mechanical zero-point fluctuation amplitude is 85 fm and the efficient mass is 0.27 zg, which is much smaller than the PhC nanobeam. The phononic superlattice-Ag nanocavity optomechanical devices hold great potential for applications in the field of integrated quantum optomechanics, quantum information, and terahertz-light transducer.

Key words: Optomechanics; phononic crystal; Ag plasmonic nanocavity; confinement; coupling

Citation: Z Y Li, H N Chang, J - M Lai, F L Song, Q F Yao, H Q Liu, H Q Ni, Z C Niu, and J Zhang, Terahertz phononic crystal in plasmonic nanocavity[J]. *J. Semicond.*, 2023, 44(8), 082901. https://doi.org/10.1088/1674-4926/44/8/082901

1. Introduction

The field of cavity optomechanics explores the interaction between electromagnetic radiation and nanomechanical or micromechanical motion[1]. Cavity optomechanics has important applications in precision measurement, regulation of macroscopic quantum properties of matter, quantum memory, and so on[2–6]. To observe quantum effects on a micromechanical element, it should first be cooled to the quantum ground state. An ultrahigh frequency THz GaAs/AlAs pillar multi-optical mode microcavity optomechanical structure has been proposed[7]. The high phonon frequency range that is obtained might even allow devices to be prepared in the quantum mechanical ground state of motion at liquid-nitrogen temperatures. Under blue-detuned driving, the photon-phonon interaction produces Stokes sidebands that correspond to phonon emission, due to an energy exchange between photons and phonons. In this process, the effective Hamiltonian has the form of two-mode squeezing, which is useful for the heralded generation of non-classical mechanical states or amplification of the mechanical motion[8]. For cavity optomechanics, to manipulate the quantum states precisely, enhance the coupling strength[9–11], reduce the thermal effect of laser, and achieve integration, it is important to reduce the volume of the optical coupling region. However, large mode volumes of GaAs/AlAs pillar multi-optical mode microcavity are hard to further reduce due to the diffraction limitation of light[9, 12, 13]. Plasmonic nano-antennas or plasmonic nano-cavities have the properties of localized surface plasmon resonances, so they can confine light into volumes far below the diffraction limit[14]. In addition, the GaAs/AlAs phononic superlattices have high adjustability, which can be used to design a narrow phononic crystal cavity. The combination of GaAs/AlAs superlattices phononic crystal and plasmonic nano-cavities is expected to reduce the mode volume and enhance the single-photon optomechanical coupling strength.

Here, we design a topological terahertz GaAs/AlAs phononic superlattice in a plasmonic nanocavity, where silver (Ag) plasmonic nanocavity is combined with GaAs/AlAs phononic crystal superlattices, as shown in Figs. 1(a) and 1(b). The phononic crystal cavity is designed to confine phonons in a range of around 4 nm in diameter. The plasmonic nanocavity with bowtie type put the phononic crystal superlattices post in the middle, which makes the optical field covered by the phonon range effective. The characteristic wavelength of the plasmonic nanocavity is designed to be 1550 nm, which has low loss in quartz fiber and has important applications in optical communication. The optical quality factor Q_c and optical mode volume V of cavity can attain 238 and 5×10^{-7} $(\lambda/n)^3$, respectively, and Q_c/V achieves 8.4×10^8 $(\lambda/n)^{-3}$, where λ is the wavelength of the light and n is the refractive index. The optomechanical single-photon coupling strength reaches 12 MHz, which is an order of magnitude higher than the conventional photonic crystal (PhC) nanobeam dielectric cavity.

Correspondence to: J Zhang, zhangjwill@semi.ac.cn
Received 13 JANUARY 2023; Revised 9 FEBRUARY 2023.

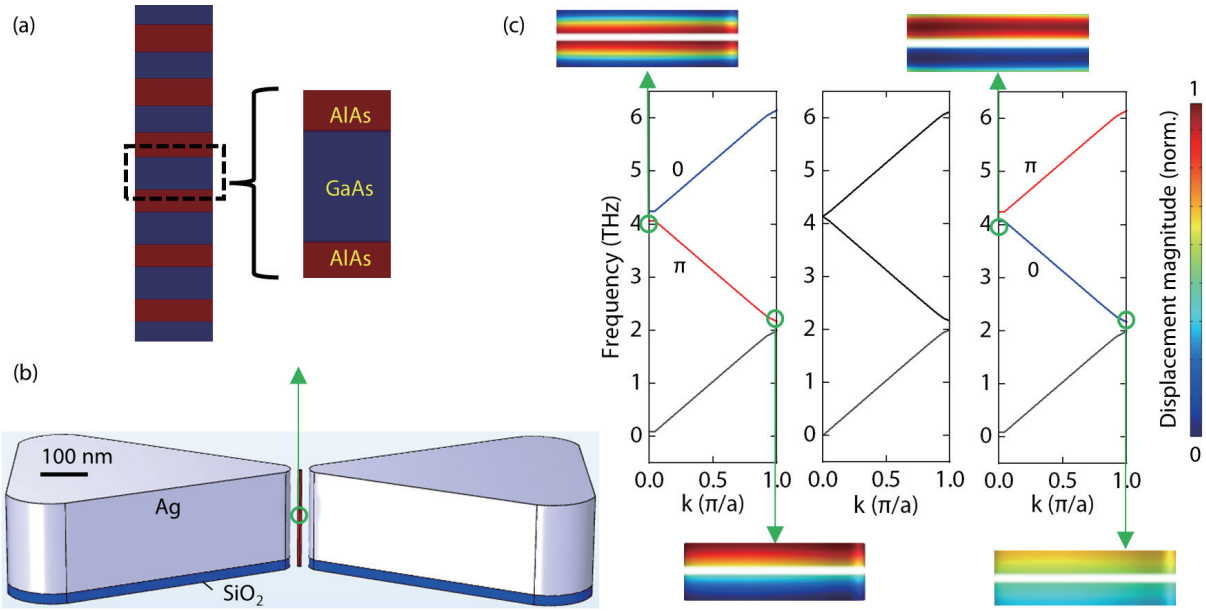

Fig. 1. (Color online) (a) Scheme of a phononic superlattice structure and its unit cell. The thickness of the upper part GaAs (AlAs) layer is different from the lower part. (b) The system composed of GaAs/AlAs phononic superlattice and bowtie Ag nanocavity with SiO_2 underneath. (c) The band inversion of GaAs/AlAs phononic superlattice δ is negative, zero, and positive from the left-hand to right-hand in the figure, respectively. The Zak phase of the middle band in each figure changes from 0 to π.

2. Confinement of Terahertz phonons in GaAs/AlAs phononic crystal

To obtain a phonon state, GaAs and AlAs occupy different proportions in the upper and lower superlattices. At a designed frequency f_0, the total acoustic path length of the unit cell is set to a half wavelength of phonons $\lambda/2$, *i.e.*, the thicknesses d of the two layers obeys $\frac{d_{GaAs}}{v_{GaAs}} + \frac{d_{AlAs}}{v_{AlAs}} = \frac{1}{2f_0}$ [15], where v is the velocity of phonons. When a phonon traverses in both layers of the cell at f_0, the accumulated phase shift is π. To describe how the overall acoustic path length is distributed between the two materials, a parameter $-1 < \delta < 1$ is defined. Keeping f_0 constant, the thicknesses of the GaAs and AlAs layers are $d_{GaAs} = \frac{v_{GaAs}}{4f_0}(1+\delta)$ and $d_{AlAs} = \frac{v_{AlAs}}{4f_0}(1-\delta)$ [15], respectively. In Fig. 1(c), we show three phonon bands corresponding to cases where δ is negative, zero, and positive and band inversion can be found. Take the middle band in each figure of Fig. 1(c) as an example: when the Zak phase is π, the band is nontrivial topological and the symmetry of modes between the center and the edge of the Brillouin region is different; when the Zak phase is 0, the band is trivial topological and the symmetry of modes between the center and the edge of the Brillouin region is the same. In this case, the reflection phases ϕ_{right} and ϕ_{left} of the upper and lower individual superlattices have to add up to an integer multiple of 2π and a stationary wave is formed. Then, a topological interface state confined between two concatenated superlattices is constructed for frequencies that fall into a bandgap for both phononic crystals. Adjusting the thickness of the superlattices, the frequency of phonons can achieve around 4 THz, which helps to realize ground-state quantum states at about 200 K. The key of phononic state confinement is to confine the topological interface phononic state in a superlattice pillar with diameters on the order of the wavelength of phonons. By reducing the diameter of the superlattices, we can limit phonons to the region of the nanometer scale.

The decrease of the diameter of the superlattices pillar has a limit, which is related to the wavelength of phonons. We know that the length of superlattices cannot be shorter than the half wavelength of phonons. Therefore, shorter wavelengths are better to confine the phonons. This is another reason why the eigenfrequency of phononic superlattices is designed as high as the minimum thickness of GaAs and the AlAs layer can be grown by molecular beam epitaxy (MBE). It should be noted that the velocity of sound is different in GaAs and AlAs, so only when the superlattice pillar diameter takes a specific value, the topological phonon states exist stably at the interface between two phononic crystals. Here, the distribution of displacement magnitude is calculated by the finite element method (FEM). The thickness of the upper and lower half GaAs/AlAs units is 0.5121/0.7412 nm and 0.6260/0.6064 nm, respectively, and the number of periods is 100. The density of GaAs and AlAs are set as 5370 and 3810 kg/m^3. Fig. 2(a) shows the distribution of the amplitude of the phonons at 4.26 THz with different superlattice pillar diameters. Fig. 2(b) further quantitatively shows the distribution of phonon amplitudes along the axial direction. There are phonons vibrating in various directions. It can be seen when diameter d takes 3.98 and 6.64 nm, there is the obvious phononic state, which distributes in the interface of phononic superlattices. While diameter d takes 3.60 nm and 5.50 nm, confinement of phonons is not good, which means that there is no stable interface state. Fig. 2(c) shows the change of ratio when the diameter takes from 3.32 to 46.50 nm. We can see when the diameter is smaller than 10 nm, the ratio periodically obtains the maximum value, and when the diameter is larger than 10 nm, the ratio is stable, which means that the interface phononic states can exist at almost every size. Therefore, when we need to confine phonons within a range that is as small as possible, the smallest diame-

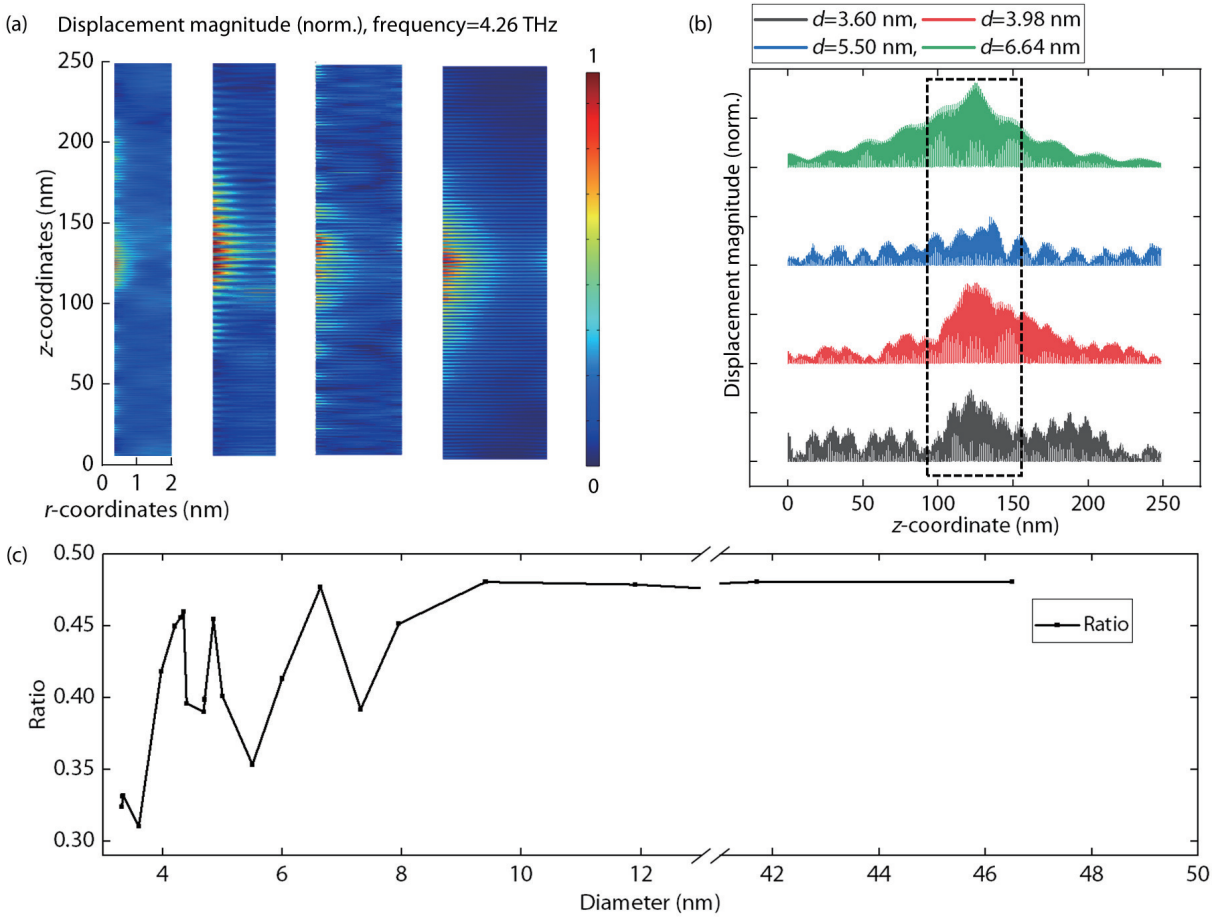

Fig. 2. (Color online) (a) The amplitude distribution of the topological interface phonons at 4.26 THz when the diameter of the superlattices pillar is at 3.60, 3.98, 5.50, and 6.64 nm. (b) The amplitude of the phonons depending on the coordinate in the axial direction (*z*-axis) at 4.26 THz. The phonon amplitudes at the *z*-axis coordinate 95–155 nm are framed in the black dotted box, where the phonon integrated amplitude is denoted as i_1. In addition, the overall phonon integrated amplitude is i_2. We define the ratio as i_1/i_2 to reflect the confinement of phonons under phononic states with different diameters. (c) The ratio depending on the diameter from 3.32 to 46.50 nm.

Table 1. The comparison of phononic frequency, Q_m, x_{zpf}, and m_{eff} between different optomechanical system.

System	PhC nanobeam[18]	Photonic DBR / Phononic superlattices[7]*	This work
Phononic frequency	~5 GHz	4.2 THz	4.2 THz
Q_m	~4.9×10^{10}	~300	2494
x_{zpf} (fm)	~0.1	0.047	85
m_{eff}	136 fg	0.92 fg	0.27 zg

* We use the structure of the reference and recalculate the relevant parameters. The same is true for the data in Tables 2 and 3.

ter is 3.98 nm. When the requirement of phonon restriction is more than 10 nm, the diameter of superlattices can be arbitrarily set according to actual needs.

We also calculate mechanical zero-point fluctuation amplitude x_{zpf} and effective mass m_{eff} of 4.26 THz phonon modes at 3.98 nm diameter. x_{zpf} is expressed as $x_{zpf} = \sqrt{\hbar/2m_{eff}\omega_m}$, where ω_m is the angular mechanical frequency. The x_{zpf} is 85 fm and the m_{eff} is 0.27 zg, which is much smaller than PhC nanobeam[16–18] and photonic distributed Bragg reflection (DBR) phononic superlattices[7] with micron level diameter, as shown in Table 1. The mechanical quality-factor Q_m is 2494, which is higher than photonic DBR/phononic superlattices[7]. The $f \times Q_m$ is around 10 PHz, which is much larger than k_BT/h with k_B being the Boltzmann and h the Planck constant at T = 300 K. This is expected to achieve quantum ground state at room temperature[19]. Furthermore, if the superlattice pillar is isolated from the substrate to eliminate dissipation, such as suspended by optical tweezers, then Q_m can theoretically reach ~10^{16} and mechanical damping rate can be reduced to ~1 mHz, reaching the minimum of the current optomechanical experiment[19].

3. Confinement and enhancement of light in Ag plasmonic nanocavity

To realize optomechanical coupling, an optical cavity that is capable of confining light and combining with phononic superlattices is required. In the design of the light cavity, the optical quality factor Q_c and mode volume V are important parameters, which represent the spectral energy density and spatial energy density of the optical microcavities. They quantitatively describe how long in time the cavity can store light and how small in space the cavity can localize light[20–22]. The light-matter interaction strength is proportional to Q_c/V, so the figure of merit Q_c/V is introduced as a basic measure to evaluate the ability of optical cavities in enhancing light-matter interaction[20, 22]. The core task is how to achieve high Q_c/V for strong light-matter interaction[14].

For our system, on the one hand, the Q_c/V of the optical

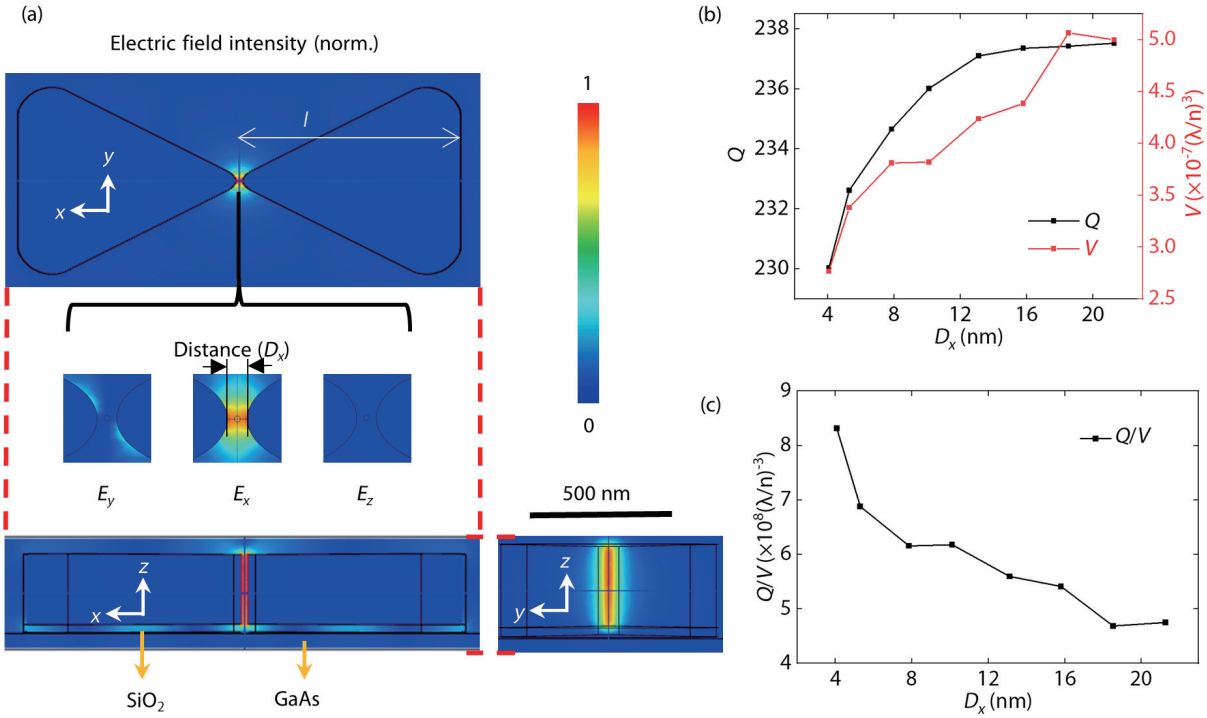

Fig. 3. (Color online) (a) The distribution of optical field in Ag nanocavity. The middle, upper and right parts are views in *x*-*z*, *x*-*y* and *y*-*z* directions, respectively. E_x, E_y, and E_z are the components of the electric field in the *x*, *y*, and *z* directions, respectively. (b) and (c) The variation of Q_c, *V*, and Q_c/V with D_x.

Table 2. Comparison of cavity wavelength, Q_c, *V*, and Q_c/V between different cavities.

System	PhC nanobeam[17, 31]	Pico-cavities[10]	Hybrid photonic-plasmonic nano-cavity[9, 14]	Photonic DBR / Phononic superlattices[7]*	This work
Cavity wavelength (nm)	~1550[17, 31]	633	1310	1550	1550
Optical *Q*-factor	~10^6[17]		9.8×10^4	45	238
Mode volume V $(\lambda/n)^3$	~0.1[31]	~1.2×10^{-7}	1.2×10^{-2}	6	2.8×10^{-7}
Q_c/V (10^8 $(\lambda/n)^{-3}$)	~0.1		0.084	7.5×10^{-8}	8.4

cavity needs to be large enough to achieve the enhancement of the optical field. On the other hand, the light field needs to be sufficient to cover the phonon field. We chose light with a wavelength of 1550 nanometers, which has important applications in light communications[17, 23–28]. However, the photonic DBR cannot confine 1550 nm light to the size of the phononic superlattice pillar with 4 nm diameter. Plasmonic nano-cavities or plasmonic nano-antennas have the properties of localized surface plasmon resonances, so they can confine light into ultra-small volumes far below the diffraction limit of light[14]. For metal plasmonic nano-cavities, the high value of Q_c/V can be realized due to the ultra-small V[14, 29, 30]. We use Ag commonly used to construct the optical cavity at 1550 nm wavelength of light[23–25]. The schematic of light field distribution is shown in Fig. 3(a) calculated by FEM, where the light is confined to the metal cavity and covers the whole phononic superlattices well. The linewidth of cavity resonance is around 0.8 THz, which is smaller than the eigenfrequency of phononic crystal. This means that the optomechanical system satisfies the resolved sideband condition.

The Ag nanocavity can carry phononic crystal superlattices with different sizes, as shown in Fig. 3(a). The distribution of different components of electric field is shown, where E_x is the strongest. For the nanocavity, the various parameters depending on the distance (D_x) of two parts of the Ag bowtie need to be investigated. In the changing of the D_x, an important point is to keep its characteristic resonant frequency at 1550 nm, so it is necessary to change the lateral size (l) of the nanocavity at the same time. We find when the characteristic wavelength of the nanocavity is kept at 1550 nm, the relationship between D_x and l satisfies $|l| = 550 + 7.66|D_x| - 0.156|D_x|^2$. The Q_c and V depending on D_x are shown in Fig. 3(b). When D_x changes from 4.07 to 21.28 nm, Q_c and V both increase. Q_c changes from 230 to 238, which is higher than reported plasmonic nanocavity[14], and V changes from 2.8 to 5.0 $\times$ 10^{-7} $(\lambda/n)^3$, which is six orders of magnitude smaller than the PhC nanobeam[16–18], on the same order of magnitude as the pico-cavity[10], and five orders of magnitude smaller than the hybrid point-defect PhC and bowtie plasmonic nanocavity[9, 14], as shown in Table 2. In the simulation, the area covered by the light field is mostly air, so n is approximately 1. Even if the optical field is mainly occupied by GaAs/AlAs superlattices, V is about 7 $\times$ 10^{-6} $(\lambda/n)^3$. From Fig. 3(c), Q_c/V is negatively correlated with D_x. Limited by the size of the phononic superlattices, the nanocavity D_x can be as small as 4.07 nm, and the corresponding Q_c/V reaches 8.4 $\times$ 10^8 $(\lambda/n)^{-3}$, which is enhanced more than 80 times with respect to the PhC nanobeam[16–18] and more than 100 times with respect to the hybrid photonic-plasmonic nanocavity[9, 14], as shown in Table 2.

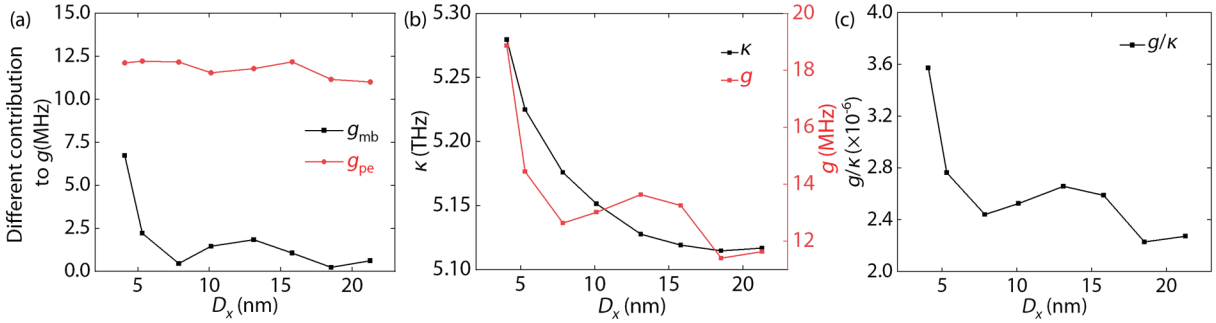

Fig. 4. (Color online) Optomechanical single-photon coupling strength (a) g_{pe} and g_{mb} depending on D_x. (b) g and κ depending on D_x. (c) g/κ depending on D_x.

4. Optomechanical coupling in phononic superlattices-Ag nanocavity system

To verify the enhancement of the optomechanical interaction, we calculate the optomechanical single-photon coupling strength g of the system. In the optomechanical cavity, the injected photons inside the cavity generate the radiation-pressure forces, including gradient forces, scattering forces, and thermal effects[1], which make a slight structural deformation around the center of the cavity. In turn, the optical field is modified by the moving dielectric boundary and the change of refractive index caused by the strain field, which is called the photo-elastic effect[32]. To quantify the interaction between photons and phonons, g is defined as[1, 17, 31]

$$g = x_{zpf} d\omega_o / da, \tag{1}$$

where a is the amplitude of the mechanical displacement field and ω_0 is the angular frequency of the optical mode. $d\omega_o/da$, calculated by first-order electromagnetic perturbation theory, demonstrates the strength of optomechanical transductions. Given the contribution of the moving dielectric boundary and the photo-elastic effect, the total optomechanical single-photon coupling strength can be written as $g = g_{mb} + g_{pe}$. The moving boundary contribution is given by[17, 31]

$$g_{mb} = -\frac{\omega_o}{2} \frac{\oint (\boldsymbol{Q}\cdot\hat{\boldsymbol{n}}) \left(\Delta\varepsilon \boldsymbol{E}_{\parallel}^2 - \Delta\varepsilon^{-1} \boldsymbol{D}_{\perp}^2\right) dS}{\int \boldsymbol{E}\cdot\boldsymbol{D} dV} x_{zpf}, \tag{2}$$

where $\hat{\boldsymbol{n}}$ is the outward facing surface normal, $\boldsymbol{Q}$ is the normalized mechanical vector displacement field (max[|$\boldsymbol{Q}$|]=1), $\boldsymbol{D}$ is the electric displacement field, $\boldsymbol{E}$ is the electric field, the subscripts $\parallel$ and $\perp$ indicate the field components parallel and perpendicular to the surface, respectively. ε is the material permittivity, $\Delta\varepsilon = \varepsilon_{material} - \varepsilon_{air}$, and $\Delta\varepsilon^{-1} = \varepsilon_{material}^{-1} - \varepsilon_{air}^{-1}$ (here, the material is GaAs or AlAs.). The photo-elastic contribution is written as[17, 31]

$$g_{pe} = -\frac{\omega_o}{2} \frac{\left\langle E \left| \frac{\partial\varepsilon}{\partial a} \right| E \right\rangle}{\int \boldsymbol{E}\cdot\boldsymbol{D} dV} x_{zpf}. \tag{3}$$

$\frac{\partial\varepsilon}{\partial a}$ is given by $\frac{d\varepsilon}{da} = -\varepsilon\left(\frac{\boldsymbol{pS}}{\varepsilon_0}\right)\varepsilon$, where $\boldsymbol{S}$ is the strain tensor and $\boldsymbol{p}$ is the rank-four photo-elastic tensor. For calculation, $\left\langle E \left| \frac{\partial\varepsilon}{\partial a} \right| E \right\rangle$ is written in terms of components:

Table 3. Comparison of phononic frequency, g_{mb}, g_{pe}, and g between different optomechanical systems.

System	PhC nanobeam[18, 31]	Photonic DBR / Phononic superlattices[7]*	This work
Phononic frequency	~5 GHz	4.2 THz	4.2 THz
g_{mb} (kHz)	~100[31]	400	600
g_{pe} (MHz)	~1[31]	3.2	11
g (MHz)	~1[18, 31]	3.6	12

$$\begin{aligned}\left\langle E \left| \frac{\partial\varepsilon}{\partial a} \right| E \right\rangle = -\varepsilon_0 n^4 \int \big[& 2Re\left\{E_x^* E_y\right\} p_{44} S_{xy} \\ & + 2Re\left\{E_x^* E_z\right\} p_{44} S_{xz} + 2Re\left\{E_y^* E_z\right\} p_{44} S_{yz} \\ & + |E_x|^2 \left(p_{11} S_{xx} + p_{12}\left(S_{yy} + S_{zz}\right)\right) \\ & + |E_y|^2 \left(p_{11} S_{yy} + p_{12}\left(S_{xx} + S_{zz}\right)\right) \\ & + |E_z|^2 \left(p_{11} S_{zz} + p_{12}\left(S_{xx} + S_{yy}\right)\right) \big] dV.\end{aligned} \tag{4}$$

The photo-elastic coefficients for GaAs are taken as (p_{11}, p_{12}, p_{44}) = (−0.165, −0.140, (p_{11}−p_{12})/2)[33–35]. We neglect the contributions of the AlAs layers to the g because the photo-elastic effect of the GaAs layers will be dominant over those of AlAs[36]. The photoelastic contribution depends mainly on the coupling of the electric field and the phonon field which are non-perpendicular. When the E_x direction is the strongest and E_y and E_z can be negligible, the phonon modes vibrating perpendicular to the x axis cannot be effectively coupled with the light field in g_{pe}, and the breathing phonon modes are fully coupled.

The influence of distance on g_{pe} and g_{mb} is shown as Fig. 4(a). Both g_{pe} and g_{mb} decrease as distance D_x increases and the photo-elastic effect contributes more to the coupling strength. In Fig. 4(b), we see g change from 12 to 18 MHz when D_x decreases and increases sharply at a small distance, which is one order of magnitude higher than PhC nanobeam[16–18], as shown in Table 3. This verifies that the plasmonic cavity greatly increased light intensity in a small area and lower D_x raises higher enhancement. Moreover, g_{pe} is mainly decided by the overlap of strain and optical fields from Eq. (3). Because the distribution of the optical field is larger than the strain field, the coverage of the optical field to the phonon field is the key to ensure sufficient coupling strength. When the full coverage is satisfied, the smaller the distance, the smaller the volume of the light field mode. On the one hand, the light field has a higher enhancement; on the other hand, the overlap of the light field and the phonon

field is improved, resulting in a higher g. In addition, the decay rate κ depending on D_x is calculated by $\kappa = \frac{\omega_0}{Q}$ also shown in Fig. 4(b). Fig. 4(c) shows the relationship between g/κ and D_x. When D_x is small, g/κ is large and κ is larger than g obviously, which means that the system has relatively high coupling strength[1] but it has not yet reached strong coupling and our calculation method can be used.

5. Conclusion

In this paper, we propose a hybrid plasmonic nanocavity and topological terahertz optomechanical system combining topological GaAs/AlAs phononic crystal superlattices vibrated at eigen phonon frequency 4.2 THz with Ag plasmonic cavity resonant at 1550 nm. By adjusting the diameter of the superlattice pillar, the phonons are confined with a diameter of ~4 nm and x_{zpf} and m_{eff} can achieve 85 fm and 0.27 zg, respectively. Ag plasmonic cavity is designed to confine the optical field and improve the overlap of the optical and mechanical modes. We get $V \sim 2.8 \times 10^{-7}\ (\lambda/n)^3$ and $Q_c/V \sim 8.4 \times 10^8\ (\lambda/n)^{-3}$, which is ~80 times that of the PhC nanobeam and ~100 times that of the hybrid photonic-plasmonic nanocavity. As a result, an optomechanical single-photon coupling strength as high as 12 MHz is obtained, which is the highest among the reported optomechanical crystal cavities in the case of non-strong coupling. The proposed phononic-plasmonic nano-cavity provides a new platform to reduce the mode volume and improve the optomechanical single-photon coupling strength, which holds great potential for applications in the field of integrated quantum optomechanics, quantum information, and terahertz-light transducer.

Acknowledgments

J. Z. acknowledges National Natural Science Foundation of China (12074371), CAS Interdisciplinary Innovation Team, Strategic Priority Research Program of Chinese Academy of Sciences (XDB28000000). and Key-Area Research and Development Program of Guangdong Province (Grant No. 2018B030329001).

References

[1] Aspelmeyer M, Kippenberg T J, Marquardt F. Cavity optomechanics. Rev Mod Phys, 2014, 86, 1391
[2] Abbott B P, Abbott R, Abbott T D, et al. Observation of gravitational waves from a binary black hole merger. Phys Rev Lett, 2016, 116, 061102
[3] Wallucks A, Marinković I, Hensen B, et al. A quantum memory at telecom wavelengths. Nat Phys, 2020, 16, 772
[4] Kuruma K, Pingault B, Chia C, et al. Coupling of a single tin-vacancy center to a photonic crystal cavity in diamond. Appl Phys Lett, 2021, 118, 230601
[5] Barzanjeh S, Xuereb A, Gröblacher S, et al. Optomechanics for quantum technologies. Nat Phys, 2022, 18, 15
[6] Zhou Z Q, Cui Y, Tan P H, et al. Optical and electrical properties of two-dimensional anisotropic materials. J Semicond, 2019, 40, 061001
[7] Chang H N, Li Z Y, Lou W K, et al. Terahertz cavity optomechanics using a topological nanophononic superlattice. Nanoscale, 2022, 14, 13046
[8] Meenehan S M. Cavity optomechanics at Millikelvin temperatures. PhD Dissertation, California Institute of Technology, 2015 (in USA)
[9] Zhang H Y, Liu Y C, Wang C Y, et al. Hybrid photonic-plasmonic nano-cavity with ultra-high Q/V. Opt Lett, 2020, 45, 4794
[10] Benz F, Schmidt M K, Dreismann A, et al. Single-molecule optomechanics in picocavities. Science, 2016, 354, 726
[11] Su R, Ghosh S, Wang J, et al. Observation of exciton polariton condensation in a perovskite lattice at room temperature. Nat Phys, 2020, 16, 301
[12] Spillane S M, Kippenberg T J, Vahala K J. Ultralow-threshold Raman laser using a spherical dielectric microcavity. Nature, 2002, 415, 621
[13] Armani D K, Kippenberg T J, Spillane S M, et al. Ultra-high-Q toroid microcavity on a chip. Nature, 2003, 421, 925
[14] Zhang H Y, Zhao W, Liu Y T, et al. Photonic-plasmonic hybrid microcavities: Physics and applications. Chin Phys B, 2021, 30, 117801
[15] Esmann M, Lamberti F R, Senellart P, et al. Topological nanophononic states by band inversion. Phys Rev B, 2018, 97, 155422
[16] Chan J, Alegre T P, Safavi-Naeini A H, et al. Laser cooling of a nanomechanical oscillator into its quantum ground state. Nature, 2011, 478, 89
[17] Chan J, Safavi-Naeini A H, Hill J T, et al. Optimized optomechanical crystal cavity with acoustic radiation shield. Appl Phys Lett, 2012, 101, 081115
[18] MacCabe G S, Ren H J, Luo J, et al. Nano-acoustic resonator with ultralong phonon lifetime. Science, 2020, 370, 840
[19] Norte R A, Moura J P, Gröblacher S. Mechanical resonators for quantum optomechanics experiments at room temperature. Phys Rev Lett, 2016, 116, 147202
[20] Vahala K J. Optical microcavities. Nature, 2003, 424, 839
[21] Asano T, Noda S. Optimization of photonic crystal nanocavities based on deep learning. Opt Express, 2018, 26, 32704
[22] Yamamoto T, Pashkin Y A, Astafiev O, et al. Demonstration of conditional gate operation using superconducting charge qubits. Nature, 2003, 425, 941
[23] Li Q, Wang S S, Chen Y T, et al. Experimental demonstration of plasmon propagation, coupling, and splitting in silver nanowire at 1550-nm wavelength. IEEE J Sel Top Quantum Electron, 2011, 17, 1107
[24] Ji Y N, Fang G Q, Shang J Y, et al. Aligned plasmonic antenna and upconversion nanoparticles toward polarization-sensitive narrowband photodetection and imaging at 1550 nm. ACS Appl Mater Interfaces, 2022, 14, 50045
[25] Kim M, Jeong C Y, Heo H, et al. Optical reflection modulation using surface plasmon resonance in a graphene-embedded hybrid plasmonic waveguide at an optical communication wavelength. Opt Lett, 2015, 40, 871
[26] Edahiro T, Horiguchi M, Chida K, et al. Spectral loss characteristics of GeO_2-P_2O_5-doped silica graded-index fibres in long-wavelength band. Electron Lett, 1979, 15, 274
[27] Henschel H, Koehn O, Schmidt H U. Radiation-induced loss of optical fibers at 1300-nm and 1550-nm wavelength. Journal, 1996, 68, 2811
[28] Mueller T, Xia F N, Avouris P. Graphene photodetectors for high-speed optical communications. Nat Photonics, 2010, 4, 297
[29] Barnes W L, Dereux A, Ebbesen T W. Surface plasmon subwavelength optics. Nature, 2003, 424, 824
[30] Holsteen A L, Raza S, Fan P Y, et al. Purcell effect for active tuning of light scattering from semiconductor optical antennas. Science, 2017, 358, 1407
[31] Li Y Z, Cui K Y, Feng X, et al. Optomechanical crystal nanobeam cavity with high optomechanical coupling rate. J Opt, 2015, 17, 045001
[32] Biegelsen D K. Photoelastic tensor of silicon and the volume dependence of the average gap. Phys Rev Lett, 1974, 32, 1196
[33] Lide D R, Bruno T J. CRC handbook of chemistry and physics. Cleveland, Ohio: CRC Press, 2012
[34] Baker C. On-chip nano-optomechanical whispering gallery resonators. PhD Dissertation, Université Paris, 2013 (in French)
[35] Chen C L. Foundations for Guided-Wave Optics. Hoboken: Wiley, 2005
[36] Lamberti F R, Yao Q, Lanco L, et al. Optomechanical properties of

GaAs/AlAs micropillar resonators operating in the 18 GHz range. Opt Express, 2017, 25, 24437

Zhenyao Li is now a M.S. student and is supervised by Prof. Jun Zhang at the State Key Laboratory of Superlattices and Microstructures, Institute of Semiconductors, Chinese Academy of Sciences. He received his Bachelor's degree from Nankai University in China. His current research interest focuses on quantum optomechanics.

Jun Zhang received his Bachelor's degree from Inner Mongolia University in China in 2004, and he received his Ph.D. from the Institute of Semiconductors, Chinese Academy of Sciences in 2010. He then worked as a postdoctoral fellow at Nanyang Technological University in Singapore from 2010 to 2015 and joined the State Key Laboratory of Superlattice for Semiconductors (CAS) as a professor in 2015. His current research focuses on light-matter interactions in semiconductor materials, including Raman and Brillouin scattering, and laser cooling in semiconductors.